Materials Science Research International, Vol.6, No.4 pp.281-286 (2000)

General paper

Neutron Diffraction Study of Thermal Residual Stress in Ceramic Composite

Yoshiaki AKINIWA*, Keisuke TANAKA*, Nobuaki MINAKAWA** and Yukio MORII**

*Department of Mechanical Engineering, Nagoya University, Furo-cho, Chikusa-ku, Nagoya 464-8603, Japan
** Japan Atomic Energy Research Institute, Tokai, Nakagun 319-1195, Japan

Abstract: The residual stress in ceramic composites of alumina mixed with various volume fractions of zirconia, Al_2O_3/ZrO_2, and of silicon carbide, Al_2O_3/SiC, was measured by the neutron diffraction method. The thermal residual stress of each constituent phase was measured as a function of the second phase. The phase stresses were determined from the neutron diffractions of ZrO_2 202, Al_2O_3 113, Al_2O_3 116 , SiC 220 and SiC 311. In Al_2O_3/ZrO_2 composites, the residual stress in the alumina phase was compression and that in the zirconia phase was tension. On the other hand, in Al_2O_3/SiC composites, the residual stress in the alumina phase was tension, and increased linearly with the silicon carbide volume fraction. The residual stresses were introduced by the mismatch of the coefficient of thermal expansion. The change of the residual stress with volume fraction of the second phase agreed well with the theoretical prediction based on Eshelby's inclusion model.

Key words: *Residual stress, Neutron stress measurement, X-ray stress measurement, Ceramic composite, Phase stress, Inclusion model*

1. INTRODUCTION

Ceramic composites have some advantages such as high fracture toughness and strength [1, 2]. Since the coefficient of thermal expansion of the second phase is different from that of matrix, the residual stress is induced during cool-down from the fabrication temperature. The residual stress has a significant effect on the mechanical properties and strength of the composites. The residual stress is different between the matrix and the second phase, so it is important to evaluate the stress state of each phase. The X-ray and neutron diffraction methods can detect separately the stress in each constituent phase of the composite. Tanaka et al. [1-4] successfully evaluated the effect of volume fraction of constituent phase on the phase stress by the X-ray diffraction method. However, X-rays measure only near-surface stress. On the other hand, neutrons are high penetrating probes, allowing the investigation of the interior of materials. Akiniwa et al. [5, 6] evaluated the phase stress in an aluminum alloy reinforced with silicon carbide particules under uniaxial loading by the neutron diffraction method.

In the present paper, the neutron diffraction method was used to measure the phase stresses in two kinds of ceramic composites. The thermal residual stresses in each constituent phase were measured by the neutron diffraction. The measured residual stress was compared with the theoretical value calculated by Eshelby's inclusion model [7, 8].

2. EXPERIMENTAL PROCEDURE

2.1. Materials and Specimens

The experimental materials used were ceramic composites of alumina mixed with various volume fractions of zirconia, Al_2O_3/ZrO_2, and of silicon carbide, Al_2O_3/SiC. The crystal structure of the alumina is the trigonal (α-Al_2O_3). The zirconia and the silicon carbide have the tetragonal structure containing 3 mol% yttria and the cubic structure (β-SiC), respectively. For the case of Al_2O_3/ZrO_2 composites, the volume fraction of zirconia is 0, 14.1, 30.4, 49.6, 72.4 and 100% as summarized in Table 1. The materials were hipped at 1450℃ for 1h under 98MPa in Ar gas. The microstructure of Al_2O_3/ZrO_2 composites is a uniform mixture of equi-axial grains of ZrO_2 and Al_2O_3 with sizes less than a micrometer [9]. The coefficient of thermal expansion (CTE) of monolithic ceramics of zirconia and alumina is 10.9×10^{-6} and 8.5×10^{-6} /℃, respectively. The CTE value of zirconia is larger than that of alumina. For the composite of Al_2O_3/SiC, the volume fraction of silicon carbide is 0, 3, 7, 14 and 26%. The composites were hipped under 40MPa. The hipping temperature was determined between 1300℃ and 1900℃ to achieve the maximum flexural

Table 1. Experimental materials.

Material	ZrO_2 content(vol%)	SiC content (vol%)
Al_2O_3/3mol% Y_2O_3-ZrO_2	0, 14.1, 30.4, 49.6, 72.4, 100	-
Al_2O_3/SiC	-	0, 7, 14, 26, 100

Received April 4, 2000
Accepted October 11, 2000
Original paper in Japanese was published in Journal of the Society of Materials Science, Japan, Vol. 49, No. 7 (2000) pp. 742-747.

Table 2. Properties of monolithic materials.

Material	Young's modulus E_M (GPa)	Poisson's ratio ν_M	Coefficient of thermal expantion α
Al_2O_3	406	0.231	8.5×10^{-6}
3mol% Y_2O_3-ZrO_2	214	0.310	10.9×10^{-6}
SiC	402	0.182	4.7×10^{-6}

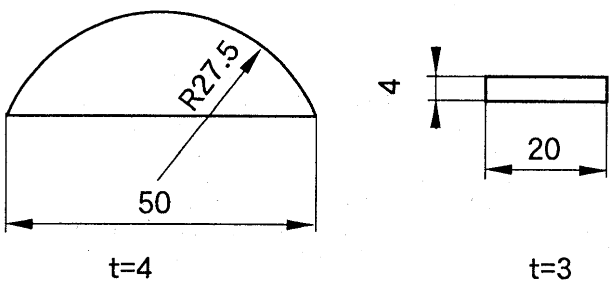

Fig. 1. Shape and dimensions of specimen.

strength. In Al_2O_3/SiC composites, nano-scale particles of silicon carbide are distributed along the grain boundary or within the grain of alumina whose size is about half to one micrometer [2]. The CTE value of monolithic silicon carbide is 4.7×10^{-6} /°C. The CTE value of silicon carbide is smaller than that of alumina. The mechanical elastic constants and the CTE of monolithic ceramics are summarized in Table 2. The elastic constants of the zirconia were experimental values [10, 11]. For the cases of alumina and silicon carbide, the values were calculated by using Kröner's model from the elastic constants of single crystals [12-14].

Figure 1 shows the shape and dimensions of the specimens. For the case of Al_2O_3/ZrO_2 composites, the bow-shaped specimen was cut off from a disk with a radius of 27.5 mm and a thickness of 4 mm. For the case of Al_2O_3/SiC composites, the rectangular specimen with a height of 4 mm, a width of 3 mm and a length of 20 mm was used.

2.2. Neutron Diffraction Measurement

The neutron stress measurement was performed for Al_2O_3 113, Al_2O_3 116, ZrO_2 202, SiC 220 and SiC 311 diffractions with the RESA (REsidual Stress Analyze equipment) at JAERI (Japan Atomic Energy Research Institute). The specimen was placed on the turntable, and rotated at 10 to 13 rpm. For the case of Al_2O_3/SiC composites, three specimens were placed on the table. The parallel beam slits were attached to receiving side of a goniometer. The slits with a height of 15 mm and a width of 10 mm were also attached to divergent and receiving sides. The irradiated volume is about 800 mm^3 for Al_2O_3/ZrO_2 composites and 540 mm^3 for Al_2O_3/SiC composites. The wave length used was 0.20995, 0.20946 and 0.20888 nm. The scanning speed was 0.1 deg/step. The preset time was determined between 30 to 600 s on the basis of the diffraction intensity. The conditions of neutron stress measurement were summarized in Table 3.

2.3. Thermal Residual Stress in Composite

The residual stress induced by the CTE mismatch has been analyzed by Taya et al. [8] on the basis of Eshelby's inclusion model [7]. The thermal residual stresses in the matrix, $\langle\sigma_m\rangle$, and in the inclusion, $\langle\sigma_p\rangle$, are given by

$$\frac{\langle\sigma_p\rangle}{E_m}=-\frac{2(1-V_f)\beta\alpha^*}{A}\ , \qquad (1)$$

$$\frac{\langle\sigma_m\rangle}{E_m}=\frac{2V_f\beta\alpha^*}{A}\ , \qquad (2)$$

where

$$A=(1-V_f)(\beta+2)(1+\nu_m)+3\beta V_f(1-\nu_m), \qquad (3)$$

$$\beta=(1+\nu_m)E_p/(1-2\nu_p)E_m\ , \qquad (4)$$

$$\alpha^*=(\alpha_p-\alpha_m)\Delta T\ . \qquad (5)$$

E_m, ν_m and α_m are Young's modulus, Poisson's ratio and CTE of the matrix, and E_p, ν_p and α_p are those of the

Table 3. Neutron diffraction conditions.

Equipment	RESA(REsidual Stress Analyzer equipment)					
Diffraction line	Al_2O_3 116	ZrO_2 202	SiC 220	SiC 311	Al_2O_3 113	Al_2O_3 116
Diffraction angle (deg)	81.94	70.5	85.62, 85.33	105.66, 105.25	60.30, 60.12	81.71, 81.43
Wave length (nm)	0.20995		0.20946, 0.20888			
Monocrometer	Si 311					
Detecter	3He-0D					
Scanning speed (deg/step)	0.1					
Preset time (sec)	40～90	40～120	240～600	240～600	30～120	30～120

inclusion. V_f and ΔT are the volume fraction of inclusion and the change of temperature, respectively.

The thermal residual stress can be regarded as equi-triaxial. Once the residual strain, ε, is obtained, the residual stress can be calculated by

$$\sigma_R = 3K\varepsilon \quad , \tag{6}$$

where K is the bulk modulus. The diffraction value of bulk modulus of alumina and silicon carbide was calculated by Kröner's model from the elastic constants of single crystals under the assumption of random orientation. For the case of zirconia, it was calculated from the mechanical elastic constants. The calculated values are summarized in Table 4.

3. EXPERIMENTAL RESULTS AND DISCUSSION

3.1. Diffraction Profile

Typical examples of the ZrO_2 202 diffraction obtained for Al_2O_3/ZrO_2 composites with the zirconia volume fraction of 14, 72 and 100 % are shown in Fig. 2(a). The preset time for the composites with V_f=14, 72 and 100 % was 120, 90 and 40 s, respectively. The profile is the doublet with ZrO_2 202 and ZrO_2 220 diffractions. Each diffraction was separated by assuming two Gaussian curves. The curves in the figure indicate the fitted results. The diffraction angle increases with the zirconia volume fraction. Figure 2(b) shows the profiles of the Al_2O_3 116 diffraction obtained for Al_2O_3/ ZrO_2 composites with V_f =0, 14 and 72 %. The preset time for the composites with V_f=0, 14 and 72 % was 40, 60 and 90 s, respectively. The data was approximated by the Gaussian curve. The diffraction angle also increases with the zirconia volume fraction.

For the case of Al_2O_3/SiC composites, the profile of SiC 220 diffraction was overlapped with the Al_2O_3 211 diffraction as shown in Fig. 3(a). The profile was obtained for the composite with the silicon carbide volume fraction of 26%. The preset time was 600 s. The diffraction angle was also determined by using the wave separation technique. Figure 3(b) shows the example of the Al_2O_3 113 diffraction. The preset time was 120 s. For the cases of Al_2O_3 113, Al_2O_3 116 and SiC 311 diffractions, the profile had a single peak.

Table 4. Bulk modulus of monolithic materials.

Diffraction plane	Bulk modulus K (GPa)
SiC 220	211.0
SiC 311	211.0
Al_2O_3 113	246.2
Al_2O_3 116	248.5
ZrO_2 202	187.7

3.2. Thermal Residual Stress

Figure 4 shows the change of the residual strain with the zirconia volume fraction obtained for Al_2O_3/ZrO_2 composites. The reference angle used to calculate the residual strain was the value obtained from hipped monolithic alumina and zirconia. For the case of the zirconia phase, the tensile residual strain was measured, because the CTE value of zirconia is larger than that of alumina. The tensile strain decreases with increasing zirconia volume fraction. On the other hand, the compressive residual strain was observed in the alumina phase. The compressive residual strain increases with the zirconia volume fraction.

Figure 5 shows the change of the residual strain with the volume fraction of the silicon carbide obtained for

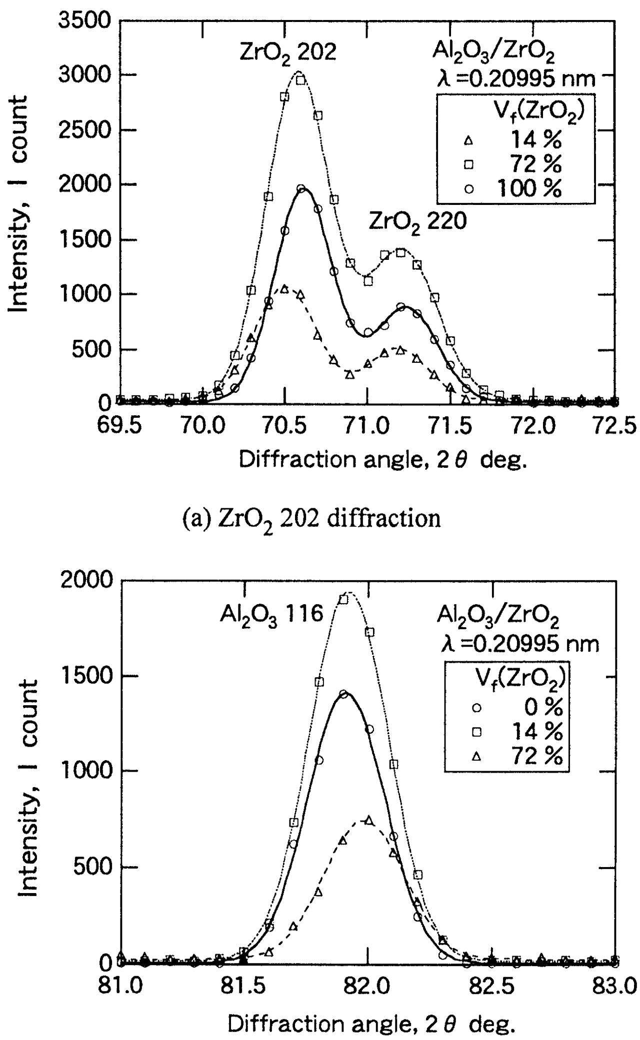

(a) ZrO_2 202 diffraction

(b) Al_2O_3 116 diffraction

Fig. 2. Neutron diffraction profiles for Al_2O_3/ZrO_2.

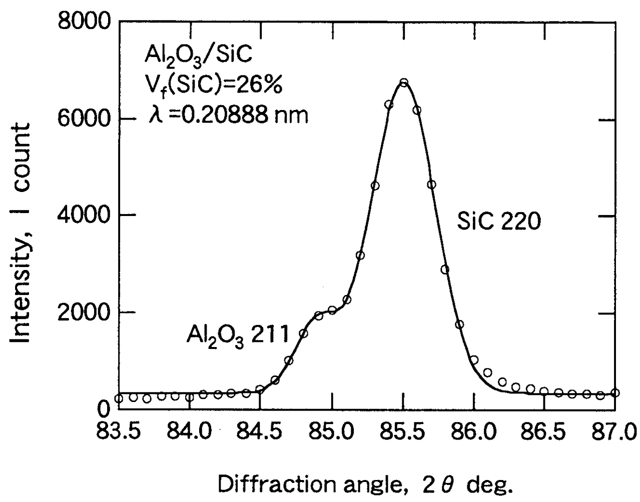

(a) SiC 220 diffraction

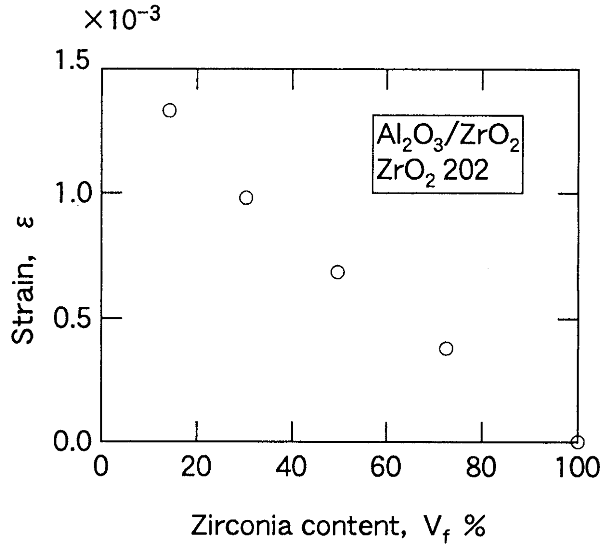

(a) ZrO_2 phase

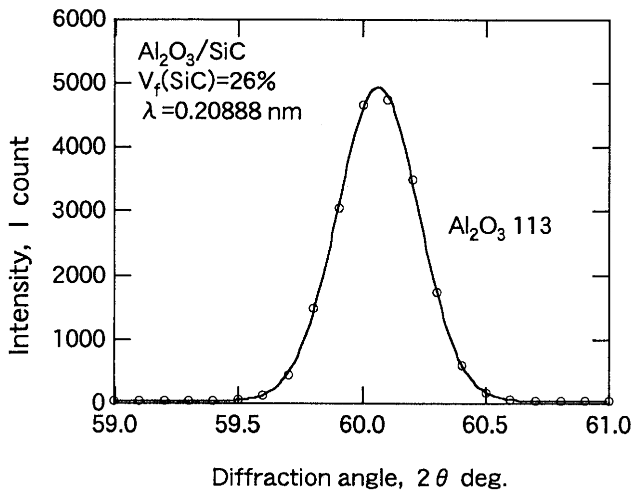

(b) Al_2O_3 113 diffraction

Fig. 3. Neutron diffraction profiles for Al_2O_3/SiC.

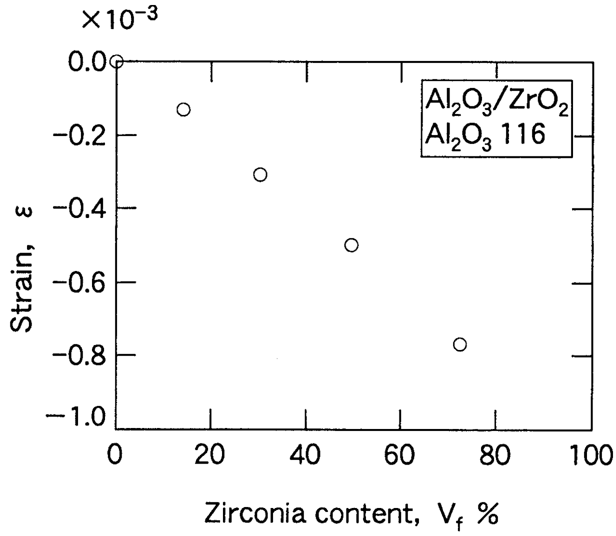

(b) Al_2O_3 phase

Fig. 4. Residual strain in Al_2O_3/ZrO_2 composites.

Al_2O_3/SiC composites. The diffraction angle measured from the silicon carbide powder was used as a reference. The residual strain in the silicon carbide phase is compression, because the CTE value of alumina is larger than that of silicon carbide. The compressive residual strain increases with the silicon carbide volume fraction. The absolute value of the compressive strain obtained for SiC 311 diffraction is larger than that for SiC 220 diffraction. On the other hand, the residual strain in the alumina phase is tension. The tensile residual strain increases with silicon carbide volume fraction.

Since the specimen was rotated on the turntable, the measured strain is the average value of the strain in the direction perpendicular to the axis of rotation. The residual strain in the direction parallel to the axis of rotation was assumed to be the same as the measured value. The residual stress was calculated by using Eq. (6). Figure 6 shows the variation of the residual stress with the zirconia volume fraction obtained for Al_2O_3/ZrO_2 composites. In the figure, the curves indicate the predicted value calculated from Eqs. (1) and (2) by regarding alumina or zirconia as the matrix phase. The composites were assumed to be subjected to a temperature change of ΔT= 1425℃. For the case of the zirconia volume fraction of 14 %, the residual stress in the zirconia phase is 750 MPa. When the volume fraction is larger than 50 %, the experimental results agree well with the prediction which is calculated as the zirconia matrix.

For the case of Al_2O_3/SiC composites, the change of the residual stress with the silicon carbide volume frac-

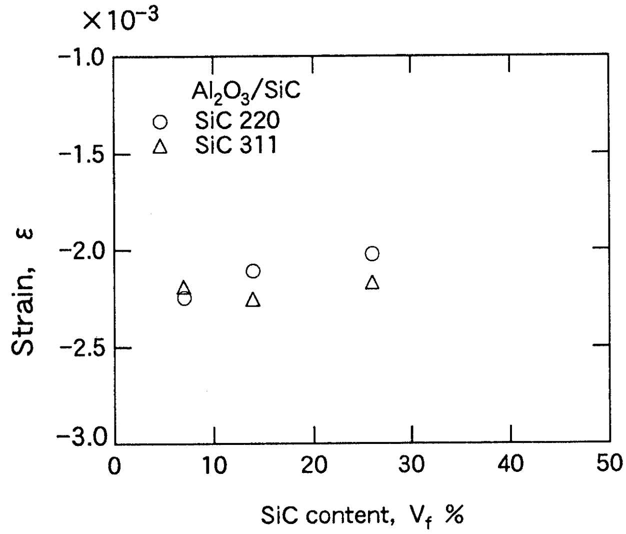

(a) SiC phase

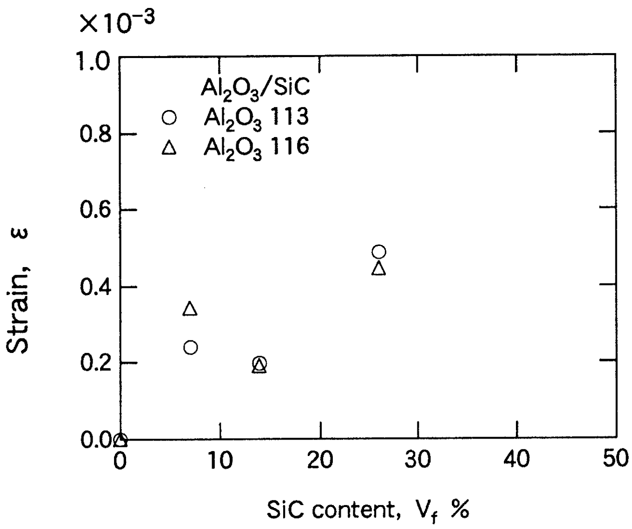

(b) Al_2O_3 phase

Fig. 5. Residual strain in Al_2O_3/SiC composites.

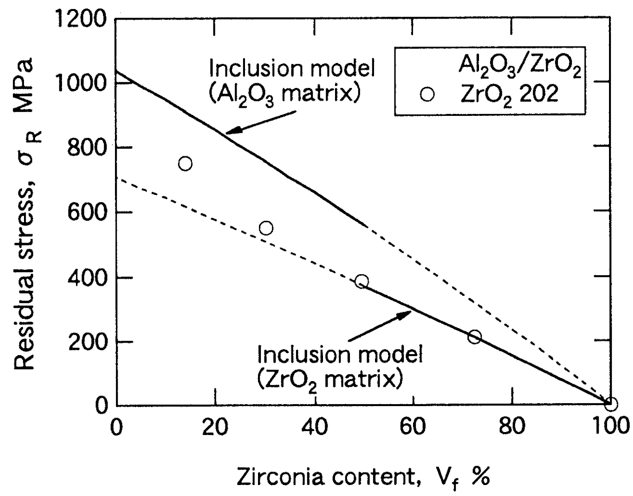

(a) ZrO_2 phase

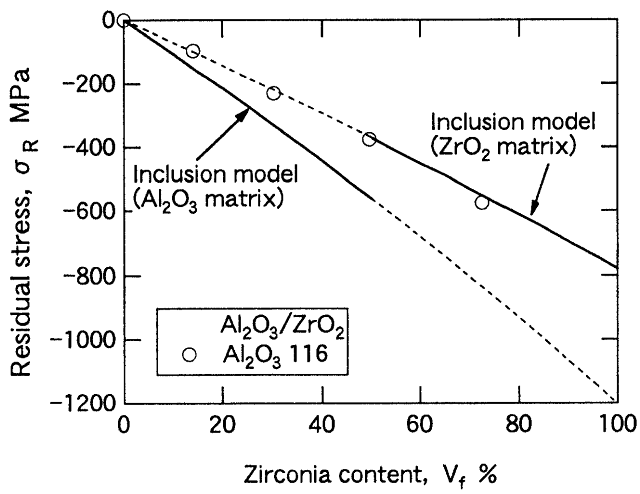

(b) Al_2O_3 phase

Fig. 6. Residual stress in Al_2O_3/ZrO_2 composites.

tion is shown in Fig. 7. The residual stresses of both phases obtained from two diffractions are close. The temperature change of ΔT =1200℃ was assumed for prediction [2]. The residual stresses in both phases agree very well with the predicted values.

When the coefficient of thermal expansion of the matrix is larger than that of inclusion, the residual stress of the matrix becomes tension. The tensile residual stress increases with the volume fraction of the inclusion. On the other hand, the compressive residual stress was introduced in the inclusion. The residual stress has a significant influence on the strength and toughness of composites [8]. The control of the residual stress plays a key role in designing ceramic composites. The neutron diffraction method is one of the most effective methods to measure them.

4. CONCLUSIONS

The thermal residual stress in ceramic composites of alumina mixed with various volume fractions of zirconia, and of silicon carbide was measured by the neutron diffraction method. The measured residual stress was compared with the predicted values calculated by Eshelby's inclusion model.

(1) When the coefficient of thermal expansion of the matrix is larger than that of inclusion, the residual stress of the matrix becomes tension. The tensile residual stress

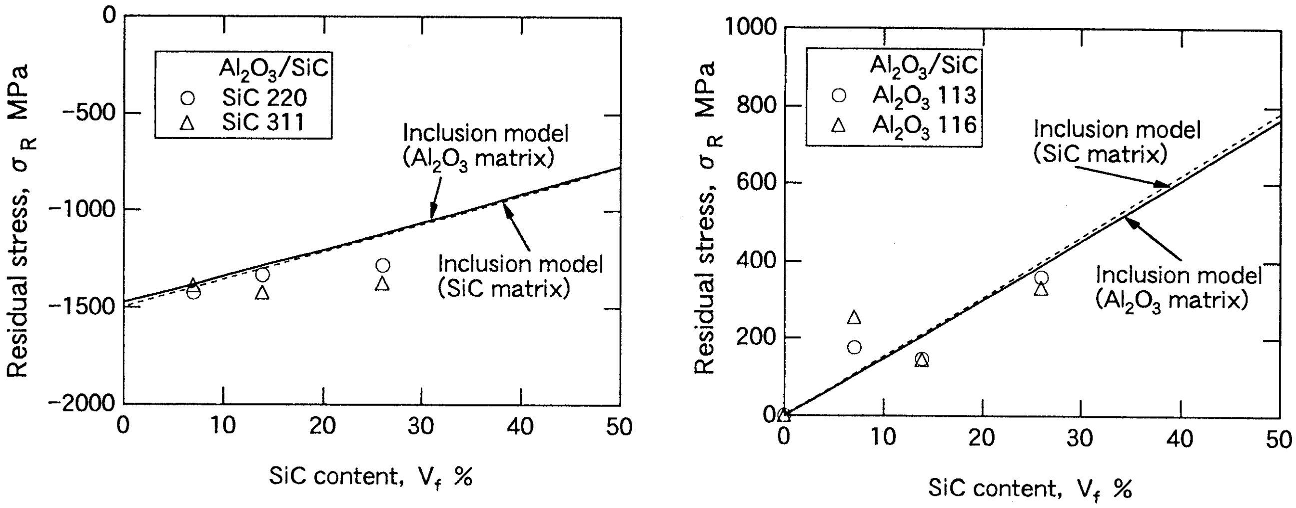

(a) SiC phase

(b) Al_2O_3 phase

Fig. 7. Residual stress in Al_2O_3/SiC composites.

increases with the volume fraction of the inclusion.

(2) For the case of the composites of alumina mixed with various volume fractions of silicon carbide, the residual stresses obtained from two different diffractions are very close.

(3) The residual stress measured by the neutron method agreed well with the theoretical prediction based on Eshelby's inclusion model.

REFERENCES

1. K. Tanaka, M. Matsui, R. Shikata and T. Nishikawa, J. Soc. Mater. Sci., Japan, **41** (1992) 593 (in Japanese).
2. J. Otsuka, S. Iio, Y. Tajima, M. Watanabe and K. Tanaka, J. Ceram. Soc., Japan, **102** (1994) 29 (in Japanese).
3. K. Tanaka, Y. Yamamoto, N. Mine, K. Suzuki and H. Nakagawa, Trans. Japan Soc. Mech. Eng., A, **56** (1990) 402 (in Japanese).
4. K. Tanaka, N. Mine, K. Suzuki, J. Soc. Mater. Sci., Japan, **39** (1990) 1235 (in Japanese).
5. Y. Akiniwa, K. Tanaka, T. Takezono, N. Minakawa and Y. Morii, Proc. 5th Int. Conf. Residual Stress, **2** (1997) 982.
6. Y. Akiniwa, K. Tanaka, T. Takezono, N. Minakawa and Y. Morii, J. Soc. Mater. Sci., Japan, **47** (1998) 755 (in Japanese).
7. J. D. Eshelby, Proc. Roy. Soc., **A241** (1957) 376.
8. M. Taya, S. Hayashi, A. S. Kobayashi and H. S. Yoon, J. Am. Ceram. Soc., **73** (1990) 1382.
9. R. Shikata, Y. Urata, T. Shiono and Y. Nishikawa, J. Japan Soc. Powder and Powder Metallurgy, **37** (1990) 357 (in Japanese).
10. K. Tanaka, Y. Yamamoto and K. Suzuki, Proc. 2nd Int. Conf. Residual Stress (1989) 382.
11. K. Tanaka, T. Kurimura, Y. Akiniwa, K. Suzuki and H. Nakagawa, Trans. Japan Soc. Mech. Eng., A, **55** (1989) 318 (in Japanese).
12. E. Kröner, Z. Phys., **151** (1958) 504.
13. W. E. Trefft, J. Res. Nat. Bur. Standard, **70A** (1966) 277.
14. K. B. Tolpygo, Soviet Phys. Solid State, **2** (1961) 2367.